THE MAIN FEATURES OF A NEW GENERATION BUILDING SIMULATION TOOL

Pekka Tuomaala
Kalevi Piira
VTT Building Technology
P.O. Box 1804, FIN-02044 VTT Finland
Pekka.Tuomaala@vtt.fi
Mika Vuolle
Helsinki University of Technology

ABSTRACT

A new generation building simulation tool combines the most important inter-acting physical processes (air infiltration and ventilation, heat transfer, and indoor air quality) in an reliable, effective, and flexible way. Here, reliability has been ensured by adopting solution routines based on the fundamental physical laws: mass balance, momentum, and heat balance equations. In addition, air flow and heat transfer calculation routines are tested by analytical and comparative test cases with other building simulation tools. An effective mathematical solution routine is adopted, and a modern object oriented programming environment is selected. These features offer new possibilities to develop fast and accurate building simulation tools for both general and special needs.

INTRODUCTION

A number of building related simulation tools have been developed during the past two decades (Liddament and Thompson 1982, Feustel and Dieris 1985, Haghighat 1989). Most of these simulation tools are dealing with building energy management (BEM), a fraction of them are capable to solve flow field problems (based on computational fluid dynamics, CFD), and some of them can predict indoor air quality (IAQ) related behaviour of buildings. A common feature with a large majority of building simulation tool available at the moment is that, instead of combining inter-active and simultaneous processes (such as heat and mass transfer, IAQ evaluation, heating and cooling system), they are more or less limited to one or two aspects at a time. Also hardware and operating system selections restrict utilization of some advanced simulation tools.

This paper presents the main features of a new generation building simulation tool. Special attention has been payed on reliability, efficiency, and flexibility of this tool. Reliability has been ensured by adopting fundamental physical equations describing all essential inter-acting prosesses (i.e. air infiltration and ventilation, and heat transfer) into an integrated simulation environment. Efficiency, and flexibility to use this new tool, are obtained by including an effective sparse matrix solution routine, and coding algorithms in an object oriented programming environment for micro computers.

METHODS

In this new building simulation tool **BUS++** (**BU**ilding **S**imulation tool coded by C++) a network assumption is adopted. This is done in order to describe a real process with a reasonable number of nodes and connections between these nodes, and to effectively obtain a numerical approximation for the problem.

This building simulation tool **BUS++** is coded in object oriented programming environment C++. Dynamic memory allocation is used in the program source code in order to use computer memory effectively, and to make it possible to simulate large networks. In the linear solver routine used in this program, only all non-zero coefficients are stored into coefficient vectors including information about the connection nodes.

Air flow simulation

Air infiltration and ventilation system simulation is based on the network approach. The nodes are connected to each other by one-dimensional flow elements. The mass balance equations of every node, and the momentum equations of each flow element are solved simultaneously. The solution is based on a fully implicit formulation of the linearized flow equations in order to obtain a stable solution. In this simulation program, wind and stack effects together with fans are included as the driving forces of air movement between nodes.

Relationship between pressure difference across a single flow element and mass flow rate through it is non-linear (except for the ideal laminar flow). Because of this non-linearity of the momentum equation, the solution has to be made iteratively. Finally, the calculation of the pressure corrections can be expressed as a linear system of equations (Tuomaala and Rahola 1995):

$$a_{ii}\Delta p_i = \sum_j a_{ij}\Delta p_j - b_i \qquad (1)$$

where

$$a_{ij} = \frac{1}{a'_{ij}}$$

$$a_{ii} = \sum_j \frac{1}{a'_{ij}} + V_i \frac{\partial \rho}{\partial p}\frac{1}{\Delta t} \qquad (2)$$

$$b_i = \frac{\sum_j R_{ij}^m}{a'_{ij}} - R_i .$$

The iteration of pressure corrections and mass flow rate corrections for each time step is continued until the residuals of mass balance equations and momentum equations are small enough (maximum mass flow rate and momentum equation residuals are, for example, less than 0.0001 kg/s and 0.01 Pa, respectively). When the convergence criteria are fulfilled, the pressures and mass flow rates for the next time step can be solved.

Heat transfer simulation

Heat transfer simulation - like air flow simulation - is based on the network approach. A heat balance method is selected for the assessment of temperature levels and energy consumption of a building. In such a method, heat loads and casual gains are applied to nodes, and heat in the process is either stored in the thermal capacities (C_i) or transferred from node *i* to node *j* (or from *j* to *i*) via a response path with conductance G_{ij} (Penman 1990). System identification consists of defining the network approximation of the building and putting numerical values to every conductance and capacitance (Clarke 1985).

A general - implicitly discretised - energy balance equation for a single node, where the mass transfer between nodes is also included, is written:

$$C_i \frac{T_i - T_i^{t-\Delta t}}{\Delta t} + \sum_j G_{ij}\left(T_i - T_j\right) + \sum_j \dot{m}_{ij}\, h_{ij} = \varnothing_i \quad , \qquad (3)$$

where

$$h_{ij} = \begin{Bmatrix} c_{pi}\, T_i^{t-\Delta t} + x_i\left(l_0 + c_{ph}\, T_i^{t-\Delta t}\right);\ \dot{m}_{ij} \ge 0 \\ c_{pi}\, T_j^{t-\Delta t} + x_j\left(l_0 + c_{ph}\, T_j^{t-\Delta t}\right);\ \dot{m}_{ij} < 0 \end{Bmatrix}, \qquad (4)$$

The superscript t - Δt refers to the previous time step, and air mass flow rates $\dot{m}_{ij}$ are obtained from air flow simulation.

Numerical methods, as described above, cause errors because of discretisation. Errors in discretisation are due to replacing the exact derivatives by approximative differences. The errors of this type cannot be totally avoided, but they can be minimised by reducing the time step in the solution, by selecting the nodes in the structure appropriately, and by planning the discretisation method carefully. In order to achieve an acceptable accuracy in transient heat flux modelling, three nodes ought to be used to describe each element of the whole structure (Clarke 1985).

Solution routine

In this new generation building simulation program one has to solve systems of linear equations that are more or less sparse. The sparsity is due to only a limited number of connections from a single node to it's adjacent nodes — coefficients between all the non-connected nodes are zero. Linear systems can be solved either directly or iteratively. When direct methods for full matricies (such as Gaussian elimination or Cholesky factorisation) are used, many elements that were zeros in the original coefficient matrix will become non-zero in the factorisation process. Such non-zero elements are called *fill-in elements* or simply *fill* (Barret et al. 1993). In general it can be wasteful to solve sparse equations using direct methods and full matrices. There are two groups of methods to solve sparse systems of linear equations efficiently. The first is to use a special version of Gaussian elimination that operates only on the non-zero elements of the coefficient matrix, and the second group of methods are the iterative solvers.

We chose to use an iterative method in the solution of the sparse linear systems. Since the matrices in our case were positive definite (symmetric and diagonally dominant), the preconditioned conjugate gradient method (PCG) could be selected. The conjugate gradient method produces iterates that are optimal in the sense that they minimise the size of the residual, $\| A\ \mathbf{x_k} - \mathbf{b} \|$, in a certain norm. The selected preconditioned conjugate algorithm is (Tuomaala and Rahola 1995):

$\mathbf{r}^0 = \mathbf{b} - A\,\mathbf{x}^0$
$M\,\mathbf{z}^0 = \mathbf{r}^0$
$\mathbf{p}^0 = \mathbf{z}^0$
$k = 0$
do
$\alpha_k = (\mathbf{r}^k, \mathbf{z}^k) / (\mathbf{p}^k, A\,\mathbf{p}^k)$
$\mathbf{x}^{k+1} = \mathbf{x}^k + \alpha_k A\,\mathbf{p}^k$
$\mathbf{r}^{k+1} = \mathbf{r}^k - \alpha_k \mathbf{p}^k$
$M\,\mathbf{z}^{k+1} = \mathbf{r}^{k+1}$
$\beta_k = (\mathbf{r}^{k+1}, \mathbf{z}^{k+1}) / (\mathbf{r}^k, \mathbf{z}^k)$
$\mathbf{p}^{k+1} = \mathbf{z}^{k+1} + \beta_k A\,\mathbf{p}^k$
$k = k + 1$
until $\| \mathbf{r}^{k+1} \| < \varepsilon$.

The major operations in the algorithm are a matrix-vector multiply $A\,\mathbf{p}^k$, inner products (e.g., $(\mathbf{r}^{k+1}, \mathbf{z}^{k+1})$), vector updates (e.g., $\mathbf{x}^{k+1} = \mathbf{x}^k + \alpha_k A\,\mathbf{p}^k$), and the preconditioning solve (solve $M\,\mathbf{z}^{k+1} = \mathbf{r}^{k+1}$ for $\mathbf{z}^{k+1}$).

We chose the following data structure for the matrix: only the non-zero values in the diagonal and upper triangular part of the matrix are stored. The non-zero values of each row of the upper triangular were stored in consecutive array locations together with the column indices. Pointers to the start of each row were stored in an addition array.

The selected solution routine (PCG) is used for solving all separately linearized sets of air flow and heat transfer equations. Inter connections between different sub processes are included by updating effects of all new iterants, and iteration loops are continued until both mass balance, momentum, and energy balance equations are simultaneously within selected convergence criteria. For example, definition of buoyancy forces is based on newly calculated node temperatures, and the latest air flow rates are adopted in the energy balance equations.

RESULTS

The first air infiltration test case is originally defined by Rao and Haghighat (1990). There is a two-storey building with four rooms and eight fixed air flow paths (Fig. 1). External wind and buoyancy are present as driving forces. Outdoor air temperature is 273 K, and indoor temperatures of 296 K and 294 K for the first and ground floor rooms, respectively. Table 1 shows constant power law air flow element flow parameters and heights from the ground level.

Table 2 shows the mass flow rates obtained by AIRNET, COMIS (Haghighat and Megri, 1997), BUS++ and ESP-r. Comparisons of the results indicate minor deviations between the simulated and analytically calculated results. Some relative differencies are quite high. However, these deviations are obtained for the flow element numbers 6 and 7, where the absolute mass flow rate deviations are quite close to the convergence criteria used in this test case.

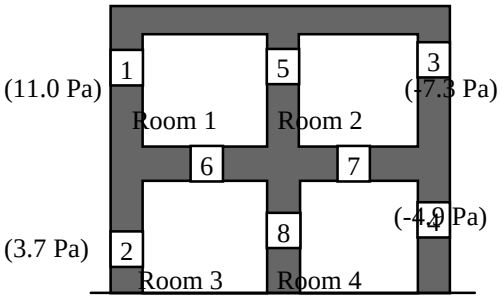

Figure 1: *Location of power law air flow elements (and external wind pressures) of the air infiltration test case(Rao and Haghighat, 1990).*

Table 1. *Power law flow element parameter values and heights from the ground level of the air infiltration test case (Rao and Haghighat, 1990).*

Flow Element	C [$m^3\ s^{-1}\ Pa^{-n}$]	n [-]	h [m]
1	0.005	0.65	5.0
2	0.008	0.65	1.0
3	0.007	0.65	5.0
4	0.009	0.65	2.0
5	0.015	0.5	5.5
6	0.020	0.5	3.0
7	0.020	0.5	3.0
8	0.015	0.5	1.5

Table 2. *Air flow elementmass flow rate values of the air infiltration test case (AIRNET and COMIS by Haghighat and Megri, 1990).*

Flow Elem.	AIRNET [$kg\ s^{-1}$]	BUS++ [$kg\ s^{-1}$]	COMIS [$kg\ s^{-1}$]	ESP-r [$kg\ s^{-1}$]
1	0.02471	0.02466	0.02437	0.02492
2	0.02760	0.02812	0.02699	0.02739
3	-0.03200	-0.03232	-0.03133	-0.03167
4	-0.02031	-0.02046	-0.02003	-0.02064
5	0.02627	0.02646	0.02597	0.02622
6	0.00157	-0.00180	0.00160	-0.00103
7	0.00573	-0.00586	0.00536	-0.00545
8	0.02604	0.02632	0.02540	0.02609

In the second air flow test case an air flow network with 12 nodes and 20 flow elements in series and parallel — originally defined by Walton (1989) — is simulated. This network (Fig. 2) is exposed to constant pressure difference of 100 Pa, and a constant air density of 1.20415 kg/m^3 is assumed.

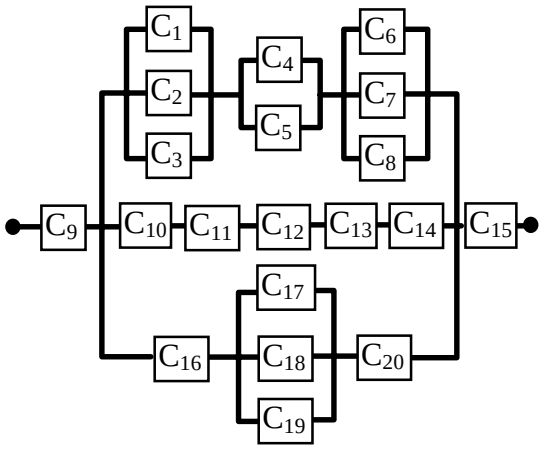

Figure 2: *Network of the Powerlaw Element Test #3. (Walton 1989)*

Table 3: *Input parameter values for airflow elements of the Powerlaw Test #3 (Walton 1989).*

Element number	Powerlaw coefficient, C_i [kg s^{-1} (kg m^{-3} Pa)$^{1/2}$
1	0.00848528
2	0.84852814
3	3.39411255
4	0.00212132
5	0.00305470
6	0.84852814
7	0.84852814
8	0.84852814
9	0.84852814
10	0.84852814
11	0.00008485
12	0.84852814
13	0.00033941
14	3.39411255
15	0.84852814
16	0.00033941
17	3.39411255
18	0.00008485
19	0.84852814
20	0.00076375

When condensing this whole network by analytical equations of flow elements (Table 3) connected in parallel and series, a reduced power law coefficient of 0.00556824 kg s^{-1} $Pa^{-0.5}$ can be obtained. In this second air flow test case, BUS++ gave a mass flow rate of 0.061102433 kg/s (i.e., 0.00006 % greater compared with the analytically calculated mass flow rate).

A heat transfer test case studied in this presentation, is a homogenious slab (Fig. 3) exposed to a step change (50 K) of external temperature (Bland 1992). The transient response is defined by both an analytical method and the studied simulation tool BUS++.

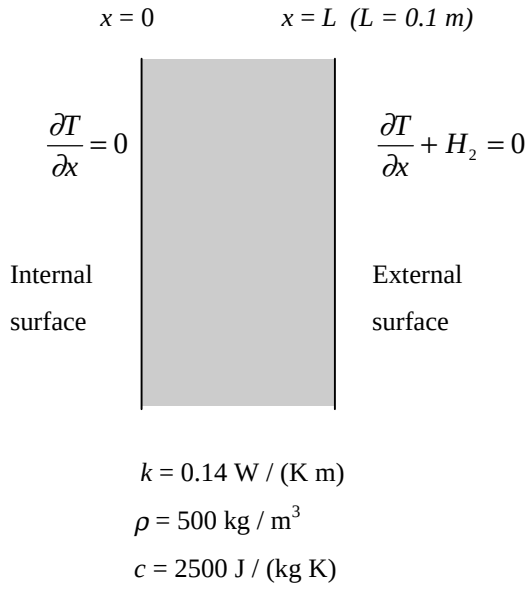

Figure 3: *A wood slab test case. (Bland 1992)*

The temperature throughout the slab is initially constant T_a = 293.15 K (20 °C), and at t = 0 the external temperature raised up to T_b = 343.15 K (70 °C). The temperature at time t and position x within the slab can be calculated from the exact solution (Özisik 1980, Bland 1992):

$$T(x,t) = T_b + 2\left(T_a - T_b\right) \sum_{m=1}^{\infty} e^{-\alpha\beta_m^2 t} \frac{H_2}{L\left(\beta_m^2 + H_2\right) + H_2} \frac{\cos(\beta_m x)}{\cos(\beta_m L)} \qquad (6)$$

where β_m are the positive roots of the transcendential equation given in Table 4.

Table 4: *Positive roots of the transcendential equation in the slab test case.*

m	β_m
1	14.6837
2	44.1279
3	73.7729
4	103.678
5	133.943
6	164.238
7	194.823
8	225.557
9	256.411

Table 5 gives analytically calculated internal and external surface temperatures and heat flux through the external surface for the first 100 hours. Figure 4 shows the temperature data in graphics for the first ten hours. The results are almost identical compared with the results given by Bland (1992). These minor differencies (0.01...0.5 %) are most likely due to different number of positive transcendential roots and sum terms included in the analytical approximation of the complete solution of the problem.

Table 5: *Analytically calculated internal and external surface temperatures and heat flux through the external surface for the first 100 hours.*

Time [h]	T_i [°C]	T_e [°C]	Q [W m^{-2}]
1	20.02191	60.678326	186.433484
2	20.846595	63.240729	135.185415
3	23.102215	64.432080	111.358405
4	26.130451	65.163988	96.720231
5	29.378996	65.686997	86.260061
6	32.576408	66.100771	77.984577
7	35.608063	66.450336	70.99329
8	38.433163	66.757245	64.855098
9	41.04396	67.032424	59.351522
10	43.446919	67.281874	54.362521
20	58.864927	68.861469	22.770628
30	65.331881	69.522698	9.546044
40	68.043001	69.799902	4.001955
50	69.179574	69.916114	1.677726
60	69.656056	69.964833	0.703347
70	69.855809	69.985257	0.294862
80	69.939551	69.993819	0.123614
90	69.974658	69.997409	0.051822
100	69.989376	69.998914	0.021725

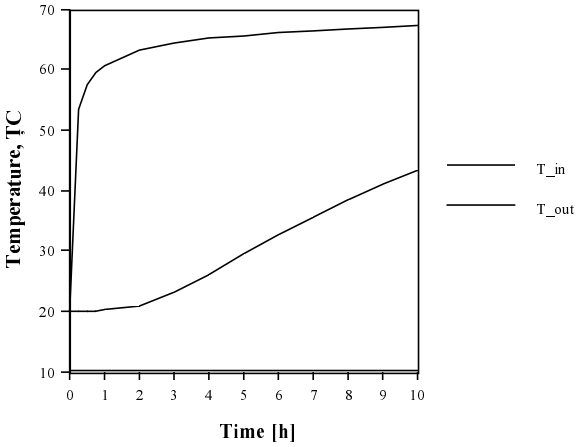

Figure 4: *Analytically solved internal and external surface temperatures of the slab test case during the period of 10 hours after the step change.*

A special discretation method of the slab test case was calculated by BUS++. Namely, an expanding grid of thermal nodes according to a geometric series was adopted. (By doing this, a strongly curvi linear temperature gradient caused by a step change can be approximated more detailed compared with, for example, the finite difference method.) In this case, the first node included such proportion of thermal mass that the Biot number of 0.05 was achieved (Δx_1 = 0.00035 m). After that the following nodes had a double thermal mass compared with there previous nodes (Δx_2 = 0.0007 m, Δx_3 = 0.0014 m, Δx_4 = 0.0028 m, Δx_5 = 0.0056 m, Δx_6 = 0.0112 m, Δx_7 = 0.0224 m, Δx_8 = 0.0448 m) — up to the last node including the rest (Δx_9 = 0.01075 m) of the whole slab thickness of 0.1m. Figure 5 presents this discretization in graphical form.

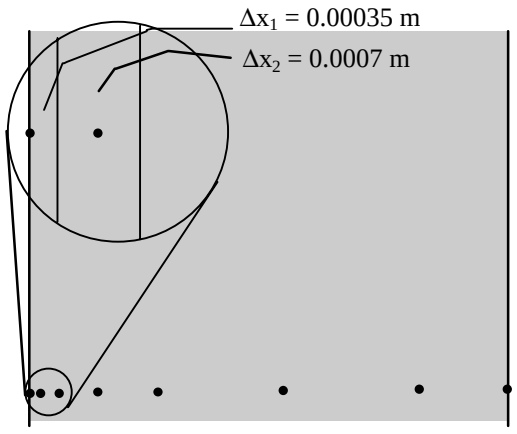

Figure 5: *Discretization of the slab test case.*

Another parameter studied, besides the non-homogenious grid generation presented above, was a time step. The time steps of 1,800 s (30 min), 900 s (15 min), and 300 s (5 min) were used. In this external temperature step change test case, the most difficult location for simulation is usually the surface node. Table 6 shows the calculated external surface node temperatures together with heat flux errors compared with the analytical solution. According to these calculations, by careful design of a thermal calculation network and selection of a time step, very reliable results can be obtained even in a rigorous step change test case as the present one.

Table 6: *Analytically solved and simulated external surface temperatures, and relative heat flux differencies after one hour from the temperature step change.*

Time step [s]	T_e [°C]	_Q/Q [%]
analytic	60.6783	-
1,800	59.2925	- 2.28
900	60.1625	- 0.85
300	60.6882	+ 0.016

CONCLUSIONS

According to air flow and heat transfer test cases, BUS++ seems to be reliable. Further development of this new generation building simulation tool is going on. Special attention is payed on improving usability of simulation facilities by developing an effective graphical user interface including parameter libraries and post-processing routines for calculation results.

A whole new area in which **BUS++** can be utilized in the near future, is evaluation of indoor air quality (IAQ). Namely, both different kinds of contaminant concentrations and thermal environment can be evaluated. In addition, living conditions of micro organisms (e.g., mould growth) can be predicted since heat and mass transfer of building materials are integrated in **BUS++**.

REFERENCES

Liddament, M. and Thompson, C. 1982. Mathematical models of air infiltration — a brief review and bibliography. Technical Note AIC 9, The *Air Infiltration Centre*, Bracknell, England.

Feustel, H. and Dieris, J. 1985. A survey of airflow models for multizone structures. *Energy and Buildings*. Vol. 18. pp 79-100.

Haghighat, F. 1989. Air infiltration and indoor air quality models — a review. *International Journal of Ambient Energy*. Vol. 10. pp 115-122.

Tuomaala, P., Rahola, J. 1995. Combined air flow and thermal simulation of buildings. *Building and Environment*. Vol. 30. pp 255-265.

Tuomaala, P., Saari K. 1994. Selection and evaluation of a thermal simulation method for a building simulatior. *Report 78. Laboratory of Applied Thermodynamics, Helsinki University of Technology*. Espoo. 28 p.

Penman, J. M. 1990. Second order system identification in the response of a working school. *Building and Environment*. Vol. 25. pp 105-110.

Clarke, J. 1985. *Energy simulation in building design*, p. 388. Bristol, Adam Higler Ltd.

Golub, G. H., Ortega, J. M. 1992. *Scientific Computing and Differential Equations - An introduction to numerical methods*, p. 337. Academic Press, San Diego USA.

Barrett, R., Berry, M., Chan, T., Demmel, J., Donato, J., Dongarra, J., Eijkhout, V., Pozo, R., Romine C., and van der Vorst, H. 1993. *Templates for the Solution of Linear Systems: Building Blocks for Iterative Methods*, p. 112. SIAM, Philadelphia USA.

Haghighat, F, Megri, A. C., 1997. A comprehensive validation of two airflow models — COMIS and CONTAM. *Indoor Air 1996*; 6: 278-288.